Systemized Structural Predesign Method for Selective Racks

Oriol Bové[1]; Miquel Casafont[2]; Miquel Ferrer[3]; Francisco López-Almansa[4]; and Francesc Roure[5]

Abstract: This paper presents a simplified stability-based method for practical structural predesign of down-aisle unbraced frames of selective racks. Given the uniformity of actual racks, only a single upright and its adjoining half beams were modeled, discretized with two-dimensional (2D) beam elements; the flexibility of the upright–beam and upright–floor connections was represented with linear springs. Such a model is used for linear buckling and second-order analyses. The proposed method consists of iteratively resizing the structural members according to cost and stability criteria (linear buckling analysis) until the serviceability limit state (SLS) and ultimate limit state (ULS) are satisfied (second order analysis). Specific procedures were developed to accelerate the computations. Two practical examples were analyzed to assess the performance of the proposed method. Compared with conventional design approaches for racks, the method was faster, and resulted in less-expensive structures. The simplification involved in the single-column consideration is sufficiently accurate. Some ideas about efficient methods of improving the stability of racks were presented. **DOI: 10.1061/(ASCE)ST.1943-541X.0002849.** © *2020 American Society of Civil Engineers.*

Author keywords: Adjustable pallet racking; Design of racks; Stability; Buckling analysis.

Introduction

Pallet rack design is not a routine task, because it depends on highly variable issues such as the size and weight of the stored goods, rack location (indoor or outdoor), rack usage (public or private), site seismicity, and so on. On the other hand, the pallet rack market is very competitive, requiring that the costs are minimized. Therefore, rack design is a crucial issue; conversely, commonly it is not highly systematized, and experience-based procedures are combined with trial-and-error approaches. Such design strategies do not always provide the cheapest and most efficient solution; furthermore, these types of design process are too slow. Thus, computer systemized approaches might be considered instead; beyond their obvious advantages, such methodologies also might be useful to find innovative solutions and to determine the cost sensitivity with respect to the design parameters (Farkas and Jarmai 2013).

Given these circumstances, this paper presents a computer systemized procedure for preliminary design of down-aisle unbraced frames of selective racks. The proposed method is practice-oriented and intuitive; Liu (2015) discussed the advantages of such practical optimization approaches. Formal optimization methods (Nocedal and Wright 2006) were not considered in this study because, although they can provide highly accurate results, the large number of involved parameters is a drawback for industrial companies needing to obtain solutions in a few seconds. The high number of parameters mainly is due to the dependence of the connection stiffness of the upright and beam sections (a third-order table of Boolean parameters must be considered to take into account the location, beam, and upright). Furthermore, some peculiarities of the cost function hinder the use of formal optimization methods. An evolution of the classical fully stressed design method (e.g., Mueller et al. 2002) was adopted. That approach, called fully drifted design, was proposed by Liu (2015); an initial design is iteratively improved until both strength and stiffness criteria are satisfied and the weight is sufficiently reduced. The proposed method also considers such criteria, but the members are resized in a different way: members that generate low cost increment and high stability gain are changed at each iteration. The proposed procedure begins with the cheapest structure that can be produced with the available steel profiles, and ends when both the strength and drift criteria are satisfied. The presented strategy is similar to the stability-based design by Manickarajah et al. (2000), although they used two-dimensional (2D) solid finite elements, whereas the present study considers beam elements. Regarding the sensitivity of stability with respect to the design parameters, the works by Perelmuter and Slivker (2001) and Szalai (2010) were used.

The proposed strategy does not consider the full down-aisle rack structure, but only a single column and its neighboring half-beams. Such a reduced model is significantly less time-consuming, and allows easier understanding of the effects of the resizing operations; this study showed that the results are sufficiently accurate for the predesign stage; the European design code

[1]Ph.D. Candidate, Dept. of Strength of Materials and Structural Engineering, Technical Univ. of Catalonia, Barcelona 08034, Spain (corresponding author). Email: oriol.bove@upc.edu

[2]Associate Professor, Dept. of Strength of Materials and Structural Engineering, Technical Univ. of Catalonia, Barcelona 08034, Spain. Email: miquel.casafont@upc.edu

[3]Associate Professor, Dept. of Strength of Materials and Structural Engineering, Technical Univ. of Catalonia, Barcelona 08034, Spain. ORCID: https://orcid.org/0000-0003-4814-0478. Email: miquel.ferrer@upc.edu

[4]Professor, Architecture Technology Dept., Technical Univ. of Catalonia, Barcelona 08034, Spain. ORCID: https://orcid.org/0000-0002-7359-110X. Email: francesc.lopez-almansa@upc.edu

[5]Professor, Dept. of Strength of Materials and Structural Engineering, Technical Univ. of Catalonia, Barcelona 08034, Spain. Email: francesc.roure@upc.edu

Note. This manuscript was submitted on December 4, 2019; approved on July 7, 2020; published online on September 24, 2020. Discussion period open until February 24, 2021; separate discussions must be submitted for individual papers. This paper is part of the ***Journal of Structural Engineering***, © ASCE, ISSN 0733-9445.

(CEN 2009) permits separate 2D analyses in the down- and cross-aisle directions, even for final design. More-complex analyses [fully three-dimensional (3D) if needed] should be performed by the designer for validation. Similar simplified models have been used in drive-in rack design (e.g., Godley 2002; Hua and Rasmussen 2006; Cheng and Wu 2015).

Apart from the reduction described in the previous paragraph, the proposed model involves other simplifications, which are described and discussed next. Load and connection eccentricities and the effect of sectional instabilities and perforations in the global analysis are not taken into account (Tilburgs 2013). However, standardized simple approaches can be implemented easily in the model to include some of the nonconsidered issues. For example, the effect of local and distortional buckling sectional deformations on member stiffness can be considered by simply reducing the cross-section properties of the beam element [the effective cross-section properties can be used in the global analysis, as proposed in EN 1993-1-3 (CEN 2019) and EN 1993-1-5 (CEN 2004)]. In a similar way, the detrimental effect of perforations on member stiffness can be accounted for by means of equivalent reduced cross-section properties, as proposed in the latest version of the EN 15512 [prEN 15512 (CEN 2016b)]. Another issue is that the structure is discretized with 2D finite elements, and therefore warping is not accounted for; their relevance for rack structures was examined by Bernuzzi et al. (2014, 2015, 2016). In this sense, the proposed model is simpler than other formulations (Trouncer and Rasmussen 2016; Sena and Rasmussen 2016) because it is intended for practical predesign. In any case, warping can be indirectly considered through the so-called warping factors defined by Bernuzzi et al. (2014, 2015). The proposed method of global analysis can be considered similar to methods accepted in current standards of cold-formed steel design: Methods 2a and 2b of prEN 15512 draft (CEN 2016b); the M3 method recently incorporated in EN 1993-1-1 and EN 1993-1-3 [EN 1993-1-3 (CEN 2019)]; and the direct analysis method of AISI (2016), which is a mixed approach combined with a B1 factor. As is demonstrated subsequently, P-Δ and sway imperfections are included in the global analysis, and the effects of torsional buckling phenomena are considered in the verification stage.

No systemized structural design approaches for rack systems have been reported to date; thus, this is one of the main contributions of this paper. Other relevant contributions are the efficient modeling of selective racks using only single-column models [even for non-totally uniform frames (Example 2)], the use of analytical expressions of the critical load factor [Eq. (11)] in terms of the design parameters, and the assessment of the sensitivity of such factor to those parameters. Noticeably, this study is computationally efficient, and thus is intended for professional daily use. In this sense, the risk of mistaking the location of different similar structural elements can be avoided by distinctive color painting or other similar easy-to-implement measures.

Future research will include first considering the warping degree of freedom, and the use of finite elements derived from the generalized beam theory (GBT). This will allow considering local and distortional buckling (Bonada et al. 2018) and accounting for the influence of the perforations (Casafont et al. 2017). The single-column model in combination with GBT is expected to be computationally effective compared with shell elements.

Pallet Rack Design

This section discusses some basic concepts of pallet rack design that are used in this paper.

Design Specifications

When a given pallet rack aisle is designed, the stored product dimensions and the maximum product weights are set by the client. Consequently, all the global rack dimensions, such as level heights, bay widths, and frame depths are part of the initial design specifications. However, these dimensions may vary slightly when the actual size of the structural profiles is considered in more-advanced stages of design. The weights of the stored goods also are known at the beginning of the design process; the only load that depends on the selected profiles is their self-weight, but this represents only a small fraction of the gravity loads. Consequently, this variation is not taken into account in a first design stage (Crosbie 1998). Additionally, all possible horizontal actions, such as seismic, forklift impact, or wind (for outdoor racks), also are quantified at the beginning. On the other hand, the global imperfection effects can be modeled either as horizontal forces or as initial sways; in this study, they are modeled as forces. Paragraph 5.3.2 of EN 15512 (CEN 2009) states that the imperfection action depends on (1) a given out-of-plumb; and (2) the looseness of the beam–upright connector. Because such looseness depends on the considered structural profiles, this imperfection action cannot be established at the initial stages of design; nevertheless, the application examples show that the presented design procedure can be initiated without knowing the final looseness. Finally, no member imperfections (initial curvature) are considered in the global analysis, as permitted in EN 15512 (CEN 2009).

The effects of seismic actions can be dealt with by representing them with equivalent static lateral forces (CEN 2016a). This rather conservative simplified approach is largely sufficient for the predesign phase.

Design Parameters

For unbraced pallet rack down-aisle structures, the main members basically are uprights (omega-shaped) and beams (box-shaped); all such elements are cold-formed. Thus, in the simplified model used for design presented herein, the in-plane upright and beam moments of inertia of each member, I_u and I_b, respectively, are the design parameters, i.e., the unknowns to be determined in the design process. Because pallet rack producers usually make their structures using a limited range of perforated steel profiles, the design problem has a finite number of design solutions.

Commonly, gross-section properties are used in global analysis, as stated in paragraph 9.2.1 of EN 15512 (CEN 2009). If more accuracy is needed, simplified approaches can be applied to account for the effect of perforations and sectional buckling phenomena on the member stiffness, such as those in prEN 15512 (CEN 2016b) and AISI (2016). In the present study, no such stiffness reduction was considered, although it could be included easily if required.

The beam-to-upright connections are a speed-lock system, thus permitting the easy positioning of any beam at any height of a regularly perforated upright. Such connections are modeled as semirigid, and their stiffness (K_{b-u}) is characterized using normative tests according to A.2.4 of EN 15512 (CEN 2009). These stiffnesses also are design parameters, but they are related to the beam and upright moments of inertia I_b and I_u; thus, the stiffnesses of the joints are not independent unknowns of the design process. The stiffnesses of the joints are considered constant. Consequently, it is not possible to reproduce any nonlinear behavior of the joints in the analysis, such as yielding. This is because, although it is feasible to implement such elastic-plastic behavior of the joints (or even the multilinear behavior) in the model, it never will be capable of reproducing in a realistic way the progressive yielding of the different joints of the structure. This is due to the fact that,

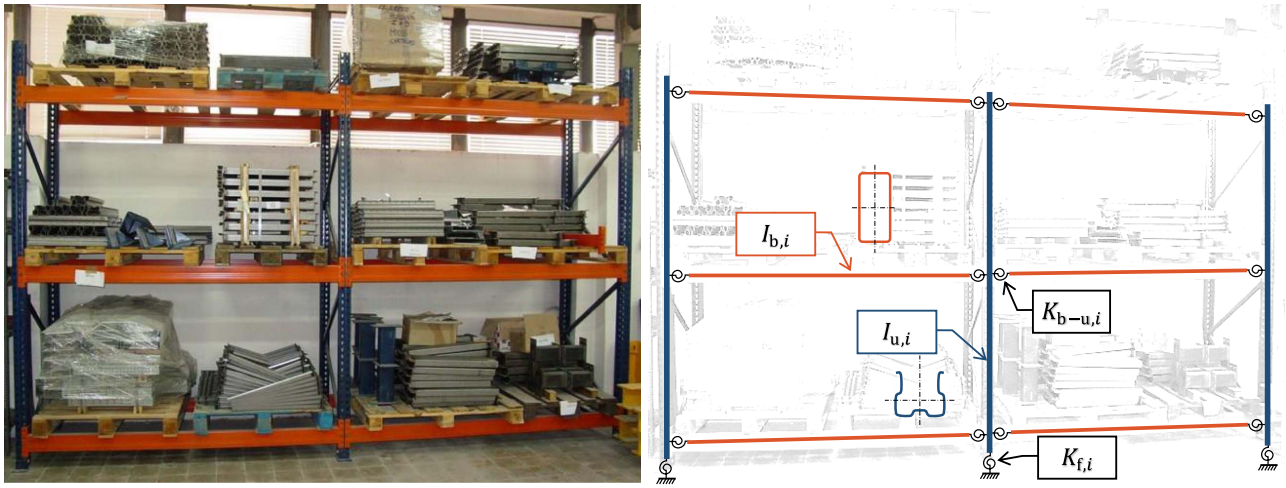

Fig. 1. Design parameters considered in the study.

as is shown subsequently, a simplified single-column model is used, which is a rather limiting factor if progressive yielding of the structure is to be modeled. On the other hand, nonlinear analyses currently are not very popular in professional practice, given that clause 9.5.4 of EN 15512 (CEN 2009) makes it extremely difficult to reach the yielding moment.

The situation is similar for the floor connections. However, in this case, their stiffness, determined according to A.2.7 of EN 15512 (CEN 2009), is a function not only of the upright moment of inertia, but also of the axial force $K_f(N)$, where N is the axial force.

All the parameters involved in the analysis are described in Fig. 1.

Design Verification

When designing a given pallet rack system, the ultimate limit state (ULS) and serviceability limit state (SLS) verifications are carried out in a similar way as for any ordinary structure. The ULS verifications are performed according to the conventional general approach (CEN 2002)

$$E_d \leq R_d \tag{1}$$

where E_d = design value of internal forces; and R_d = resistance design value. In the design method presented herein, E_d is obtained from a simplified analysis model, and R_d is determined from experimental tests carried out according to EN 15512 (CEN 2009). The considered tests are (1) stub column tests (to obtain the effective sectional properties accounting for the perforations), (2) distortional buckling tests (to obtain the distortional buckling effective area), (3) frame compression tests (to account for the global buckling), (4) upright bending tests (to determine the effective sectional flexural parameters and the lateral torsional buckling strength), (5) beam bending tests (for a similar purpose), (6) beam–upright connection tests (to obtain their stiffness, moment, and shear capacity), and (7) floor connection tests (to determine the bending stiffness and resistances for different levels of axial compression).

Although a verification scheme based on experimental tests was adopted in this study, the proposed design procedure easily can be adapted to R_d values derived from analytical calculations.

For the SLS verification, the following condition should be fulfilled (CEN 2002):

$$E_d \leq C_d \tag{2}$$

where E_d = horizontal displacements at each level of rack; and C_d = limiting values defined in EN 15512 (CEN 2009).

Pallet Racks Considered in This Study

A given pallet rack aisle can have a very great variety of beams and uprights and can be very irregular in beam level heights and bay widths. This is because the stored products can be very diverse in dimensions and weight, and hence each part of the rack must be designed accordingly. However, this situation is not the most common, especially in long aisles, because usually the goods are stored following certain sorting criteria; thus, some regularity normally is assumed. Thus, this paper focused on structures fulfilling the following conditions:

- In the down-aisle direction, the rack dimensions, loads, and structural members are uniform (Fig. 2). However, certain irregularities are considered (Example 2).
- The relative heights between levels are not necessarily equal.
- The loads in the different levels are not uniform.
- No braces are used in the down-aisle direction.

One of the justifications of this vertical nonregularity is that sometimes the lowest levels should be more accessible to people, as when they are reserved for picking, and hence are shorter than the higher levels (which are employed for heavier unit loads, such as pallets). Furthermore, in racks with forklifts, the top beam levels are higher than the bottom beam levels (CEN 2008); the aim is to leave more maneuverability space. Conversely, there is uniformity in the down-aisle direction, because the stored products are the same.

Annex C of EN 15512 (CEN 2009) contains structural design criteria for regular racks; however, these criteria are intended for racks that use the same beam profile in all their levels. Conversely, the structures studied in this paper can have different beam profiles at different levels, even with the same load. This irregularity is due to the relevant contribution of the beams to the lateral stability of the rack. In this sense, in any moment-resisting frame, lateral resistance (and thus stability) is very necessary to withstand seismic, wind, forklift impact, and global imperfection effects. Such resistance is best provided by bracing; however, in some situations bracing is not possible, mainly due to space restrains. In pallet racks, braces can be installed easily in the cross-aisle direction but not in the down-aisle direction. The reason is that the front space must be kept clear to allow easy unit placing, and installing braces only in

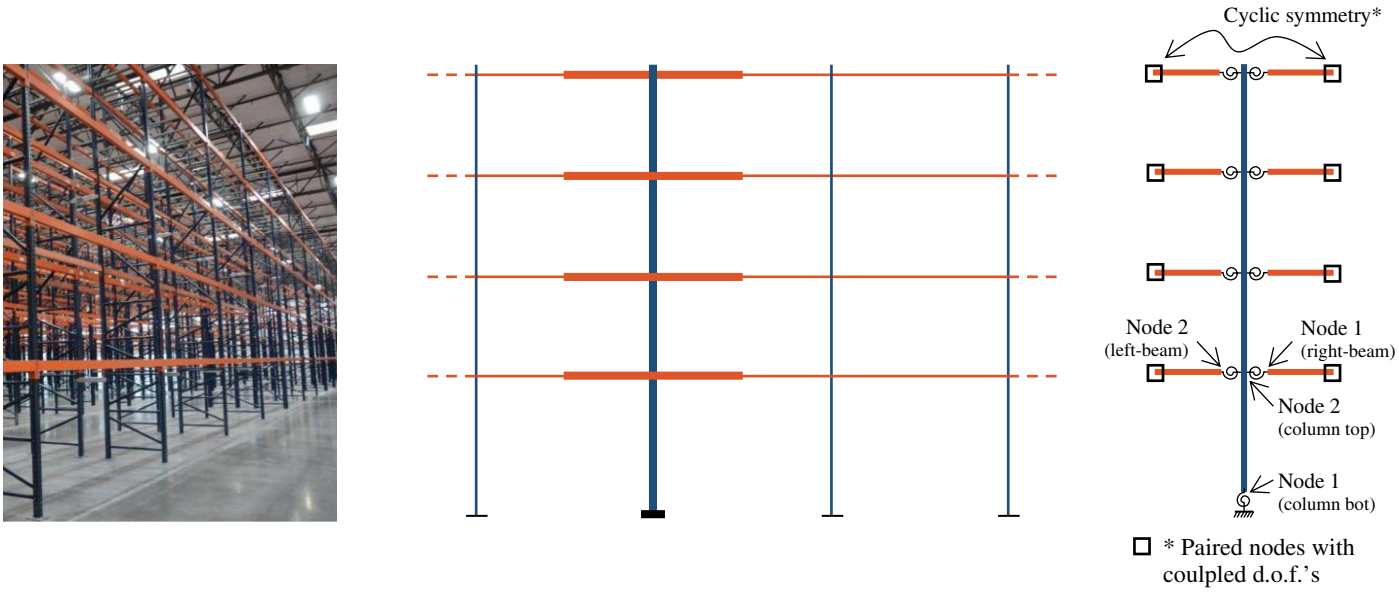

Fig. 2. Pallet rack structure and single-column model.

the rear space would lead to highly prejudicial torsion effects. Hence, ordinarily, pallet racks are braced only in the cross-aisle direction; as a consequence, the stability in the down-aisle direction becomes a major design issue. Therefore, structures without down-aisle bracings were considered in this study, and they were oriented to avoid bracing while limiting the need for stiffening the structural members and connections (Tilburgs 2013).

Down-Aisle Single-Column Model

A 2D simplified finite-element frame model of the rack was developed. Due to the horizontal uniformity of the structure, a single upright and its neighboring half-beams are included in the model (Fig. 2); the members are discretized with 2-node beam elements. A linear spring at the bottom of the upright is introduced to represent the semirigid floor connection, and linear springs also are incorporated in the beam–upright connections. To impose the periodic condition in the finite-element model, all the degrees of freedom (displacements and rotations) at the end of the modeled half-beams of each level are coupled (Fig. 2). Given the high axial stiffness of the members, the vertical displacements of the upright nodes are suppressed; they are not needed to determine approximately the upright's axial compression, because (neglecting the influence of the beams bending moments) it can be calculated by summing the vertical loads. For the beams, all the degrees of freedom are considered, except the vertical displacement that is shared with the upright.

The linear and geometric stiffness matrices are listed in Table 1 for clarification. Because the axial loads in the uprights are known, their geometric stiffness matrix can be set directly. A preliminary analysis is not carried out to determine the axial load distribution within the structure. Because there is no bracing, the axial forces in the beams are neglected.

This simplified model obtain the buckling loads of the rack using the following eigenvalue problem:

$$(\mathbf{K} + \alpha_b \mathbf{K}_G)\boldsymbol{\phi}_b = 0 \tag{3}$$

where $\mathbf{K}$ = initial (linear) stiffness matrix; $\mathbf{K}_G$ = geometric stiffness matrix; α_b = global dimensionless buckling factors (stability

Table 1. Stiffness matrices

Description	Matrix
Upright elastic matrix	$\mathbf{K}^e = \begin{bmatrix} -\frac{12EI_u}{L^3} & -\frac{6EI_u}{L^2} & -\frac{12EI_u}{L^3} & -\frac{6EI_u}{L^2} \\ -\frac{6EI_u}{L^2} & -\frac{4EI_u}{L} & -\frac{6EI_u}{L^2} & -\frac{2EI_u}{L} \\ -\frac{12EI_u}{L^3} & -\frac{6EI_u}{L^2} & -\frac{12EI_u}{L^3} & -\frac{6EI_u}{L^2} \\ -\frac{6EI_u}{L^2} & -\frac{2EI_u}{L} & -\frac{6EI_u}{L^2} & -\frac{4EI_u}{L} \end{bmatrix}$
Upright geometric matrix	$\mathbf{K}_G^e = \begin{bmatrix} -\frac{6N}{5L} & -\frac{N}{10} & -\frac{6N}{5L} & -\frac{N}{10} \\ -\frac{N}{10} & -\frac{2LN}{15} & -\frac{N}{10} & -\frac{LN}{30} \\ -\frac{6N}{5L} & -\frac{N}{10} & -\frac{6N}{5L} & -\frac{N}{10} \\ -\frac{N}{10} & -\frac{LN}{30} & -\frac{N}{10} & -\frac{2LN}{15} \end{bmatrix}$
Beam matrix	$\mathbf{K}^e = \begin{bmatrix} -\frac{A_bE}{L} & 0 & 0 & -\frac{A_bE}{L} & 0 & 0 \\ 0 & -\frac{12EI_b}{L^3} & -\frac{6EI_b}{L^2} & 0 & -\frac{12EI_b}{L^3} & -\frac{6EI_b}{L^2} \\ 0 & -\frac{6EI_b}{L^2} & -\frac{4EI_b}{L} & 0 & -\frac{6EI_b}{L^2} & -\frac{2EI_b}{L} \\ -\frac{A_bE}{L} & 0 & 0 & -\frac{A_bE}{L} & 0 & 0 \\ 0 & -\frac{12EI_b}{L^3} & -\frac{6EI_b}{L^2} & 0 & -\frac{12EI_b}{L^3} & -\frac{6EI_b}{L^2} \\ 0 & -\frac{6EI_b}{L^2} & -\frac{6EI_b}{L} & 0 & -\frac{6EI_b}{L^2} & -\frac{4EI_b}{L} \end{bmatrix}$
Rotational spring matrix	$\mathbf{K}^e = \begin{bmatrix} -k_r & -k_r \\ -k_r & -k_r \end{bmatrix}$

factors); and $\boldsymbol{\phi}_b$ = buckling modes. In a similar way, second-order analyses can be performed as

$$(\mathbf{K} + \mathbf{K}_G)\boldsymbol{\phi} = \mathbf{F} \tag{4}$$

where $\boldsymbol{\phi}$ and $\mathbf{F}$ = displacement and external force vectors, respectively.

Given the aforementioned simplifications, the model results are not exact, but can be used as an approximation; the accuracy compared with that of 2D finite element models of the whole structure is assessed at the end of this paper.

Design Strategy

The lateral stability of racks is a nonlinear problem, with material and geometric nonlinearities; nevertheless, the critical (lowest) sway stability factor, α_{cr}, is widely used in early design stages. This is because any increment of α_{cr} yields higher nonlinear ultimate loads. Thus, the sensitivity of α_{cr} to the design parameters can indicate how to improve the ultimate load. Commonly, actual pallet racks are designed for low values of α_{cr}, in many cases lower than 2. For such low values, the second-order moments and lateral displacements become high compared with the first-order moments; however, they can be significantly decreased with a small increase of α_{cr}. This study aimed to improve the pallet racks behavior by increasing α_{cr}.

When α_{cr} is greater than 10, EN 1993-1-1 (CEN 2005) permits using linear analysis, because the global second-order effects are not relevant. Thus, in this study, the improvement of the linear stability makes sense only when α_{cr} is less than 10. For high values of the stability factor, a design procedure based on the individual member strength and stiffness, such as the fully drifted design (Liu 2015), would be more suitable. On the other hand, when α_{cr} is less than or equal to 1 the structure becomes unstable; thus, it is recommended to begin with any $\alpha_{\text{cr}}^{\text{min}} > 1$. The α_{cr} of a given pallet rack never decreases when a single parameter of the linear stiffness matrix increases; as a result, the considered structures do not exhibit relative extrema (maximum or minimum) in terms of linear stability.

The gradient of α_{cr}, $\nabla\alpha_{\text{cr}}$, describes the variation of stability with respect to the design parameters $I_{u,i}$, $I_{b,i}$, $K_{b-u,i}$, and $K_{f,i}$, where subscript i indicates a member (either upright or beam) or a joint (either beam–upright or upright–base connections). Consequently, the gradient of α_{cr} helps to identify which members of the structure contribute the most to increase the stability. Thus, a stability-based design procedure may be set in which a path of gradient-oriented solutions leads to the final one; however, a slightly different approach was considered by also incorporating the cost of the structure.

Derivation of Stability Factor Gradient for Single-Column Model

The element linear stiffness matrix used in the analysis (Table 1) has linear dependence on the design parameters $I_{u,i}$, $I_{b,i}$, $K_{b-u,i}$, and $K_{f,i}$. If, for simplicity, these parameters are referred to as $\boldsymbol{\psi} = (\psi_1, \ldots, \psi_n)$, then the global stiffness matrix of the single-column model can be written

$$\mathbf{K} = \mathbf{K}^{(\mathbf{0})} + \sum_{i=1,\ldots,n} \psi_i \mathbf{K}^{(i)} \tag{5}$$

where $\mathbf{K}^{(0)}$ includes the assembled terms of the linear stiffness matrix that do not depend on the design parameters, namely the cross-sectional area of the beams; and $\mathbf{K}^{(i)}$ easily can be derived for each finite element (upright, beam, or rotational stiffness) from Table 1. Because the internal forces of the structure are obtained directly from the external loads, the geometric stiffness matrix $\mathbf{K}_G$ can be assumed to be constant.

The gradient of the stability factor can be obtained from the derivative with respect to the design parameters ψ_i of the following expression obtained from Eq. (3) (Manickarajah et al. 2000):

$$\boldsymbol{\phi}_{\text{cr}}^{\text{T}}(\mathbf{K} + \alpha_{\text{cr}}\mathbf{K}_G)\boldsymbol{\phi}_{\text{cr}} = \boldsymbol{\phi}_{\text{cr}}^{T}0 = 0 \tag{6}$$

Due to the linear nature of the relationship between the design parameters and the terms in Eq. (6), its derivation becomes straightforward and results in

$$\nabla\alpha_{\text{cr}} = \left(\frac{\partial\alpha_{\text{cr}}}{\partial\psi_1} \cdots \frac{\partial\alpha_{\text{cr}}}{\partial\psi_n}\right)^{\text{T}} \tag{7}$$

where

$$\frac{\partial\alpha_{\text{cr}}}{\partial\psi_i} = \frac{\boldsymbol{\phi}_b^{\text{T}}\mathbf{K}^{(i)}\boldsymbol{\phi}_b}{\boldsymbol{\phi}_b^{\text{T}}\mathbf{K}_G\boldsymbol{\phi}_b} \tag{8}$$

As discussed in the previous section, these partial derivatives with respect to the different parameters can be used to determine which member is the best to replace to improve the critical load of the structure. The following parameter is defined to quantify the influence of changing a specific member (Szalai 2010):

$$SIm_i = 100\frac{\frac{\partial\alpha_{\text{cr}}}{\partial I_i}}{\sum_j \frac{\partial\alpha_{\text{cr}}}{\partial I_j}} = 100\frac{\boldsymbol{\phi}_b^{\text{T}}\mathbf{K}^{(i)}\boldsymbol{\phi}_b}{\sum_j \boldsymbol{\phi}_b^{\text{T}}\mathbf{K}^{(j)}\boldsymbol{\phi}_b} \tag{9}$$

where SIm_i = parameter sensitivity indicator corresponding to member i (%), where the summation in the denominator includes all the members, but not the joints. A similar parameter can be defined for the rotational springs

$$SIr_i = 100\frac{\frac{\partial\alpha_{\text{cr}}}{\partial Ks_i}}{\sum_j \frac{\partial\alpha_{\text{cr}}}{\partial Ks_j}} = 100\frac{\boldsymbol{\phi}_b^{\text{T}}\mathbf{K}^{(i)}\boldsymbol{\phi}_b}{\sum_j \boldsymbol{\phi}_b^{\text{T}}\mathbf{K}^{(j)}\boldsymbol{\phi}_b} \tag{10}$$

where SIr_i = parameter influence indicator corresponding to rotational stiffness i, where the summation in the denominator includes all the joints, but not the members. The members and joints are treated separately because the moments of inertia ($I_{u,i}$ and $I_{b,i}$) and the rotational springs ($K_{b-u,i}$ and $K_{f,i}$) have different dimensional units. The subsequent design examples show that the SIm_i and SIr_i parameters can be very useful to the designer to understand the global behavior of a rack structure and the evolution of its design toward the best solution. As discussed previously, the rotational stiffness is not actually independent design parameters of the structure due to its dependence on the members that are connected to the joint. The rotational stiffness is determined experimentally for each particular upright–beam set or upright–base connection. Conversely, there is no mathematical relationship between the member design parameters, $I_{u,i}$ and $I_{b,i}$, and the rotational stiffness of the corresponding associated joint. Consequently, the derivatives of α_{cr} with respect to $K_{b-u,i}$ (or $K_{f,i}$), as well as SIr_i, have to be calculated independently of the member design parameters.

Critical Load Factor Approximation Using FEM

The second-order Taylor approximation of $\alpha_{\text{cr}}(\boldsymbol{\psi})$ is used to determine the critical load factor

$$\alpha_{\mathrm{cr}} \approx Q_{\alpha} = \alpha_{\mathrm{cr}}(\boldsymbol{\psi}_0) + \nabla\alpha_{\mathrm{cr}}(\boldsymbol{\psi} - \boldsymbol{\psi}_0) + \frac{1}{2}(\boldsymbol{\psi} - \boldsymbol{\psi}_0)^{\mathrm{T}}\mathbf{H}(\boldsymbol{\psi} - \boldsymbol{\psi}_0) \tag{11}$$

where $\boldsymbol{\psi}_0$ = vector of design parameters corresponding to a solution with a known stability factor; $\boldsymbol{\psi}$ = vector of design parameters corresponding to another solution; and $\mathbf{H}$ = Hessian matrix with components

$$H_{ij} = \frac{\partial^2 \alpha_{\mathrm{cr}}}{\partial\psi_i \partial\psi_j} = 2\frac{\boldsymbol{\phi}_b^{\mathrm{T}}\left(\mathbf{K}^{(i)} + \frac{\partial\alpha}{\partial\psi_i}\mathbf{K}_G\right)\frac{\partial\boldsymbol{\phi}_b}{\partial\psi_j}}{\boldsymbol{\phi}_b^{\mathrm{T}}\mathbf{K}_G\boldsymbol{\phi}_b} \tag{12}$$

$$\frac{\partial\phi_b}{\partial\psi_j} = (\mathbf{K} - \alpha_{\mathrm{cr}}\mathbf{K}_G)^{-1}\left(-\mathbf{K}^{(j)} - \frac{\partial\alpha_{\mathrm{cr}}}{\partial\psi_j}\mathbf{K}_G\right)\boldsymbol{\phi}_b \tag{13}$$

From the computation point of view, the calculation of the stability factor trough Eq. (11) for all the possible solutions (or for a given group of possible solutions) is much less time-consuming than solving Eq. (3). This prediction of the critical load factor for any structure is possible without creating and assembling the stiffness matrix at each iteration, because the value of $Q_{\alpha}(\boldsymbol{\psi})$ is calculated with a simple formula. Therefore, Eq. (11) is applied in the design algorithm presented in the next section. A Taylor linear approximation was tried instead of Eq. (11), but it did not work properly.

Design Algorithm

A design algorithm is proposed; its objective is to obtain a structure that verifies the code ULS and SLS criteria at the minimum economic cost. The critical load factor prediction presented previously is used to make decisions in the final solution search.

The design algorithm (Fig. 3) starts by setting an initial solution, S_0. This solution may be the cheapest one that can be produced with the available profiles, or the cheapest solution derived from some preliminary verifications. For instance, the beam profiles can be selected by carrying out simplified calculations which estimate and verify bending moments. This will remove part of the possible solutions, usually nonsense, and make the process more efficient.

Next, the remaining possible solutions S_i are arranged by cost $[C(S_i)]$, from lowest to highest: $C(S_0) < \cdots < C(S_n)$. Afterward, the critical load factor α_{cr} corresponding to S_0 is determined by

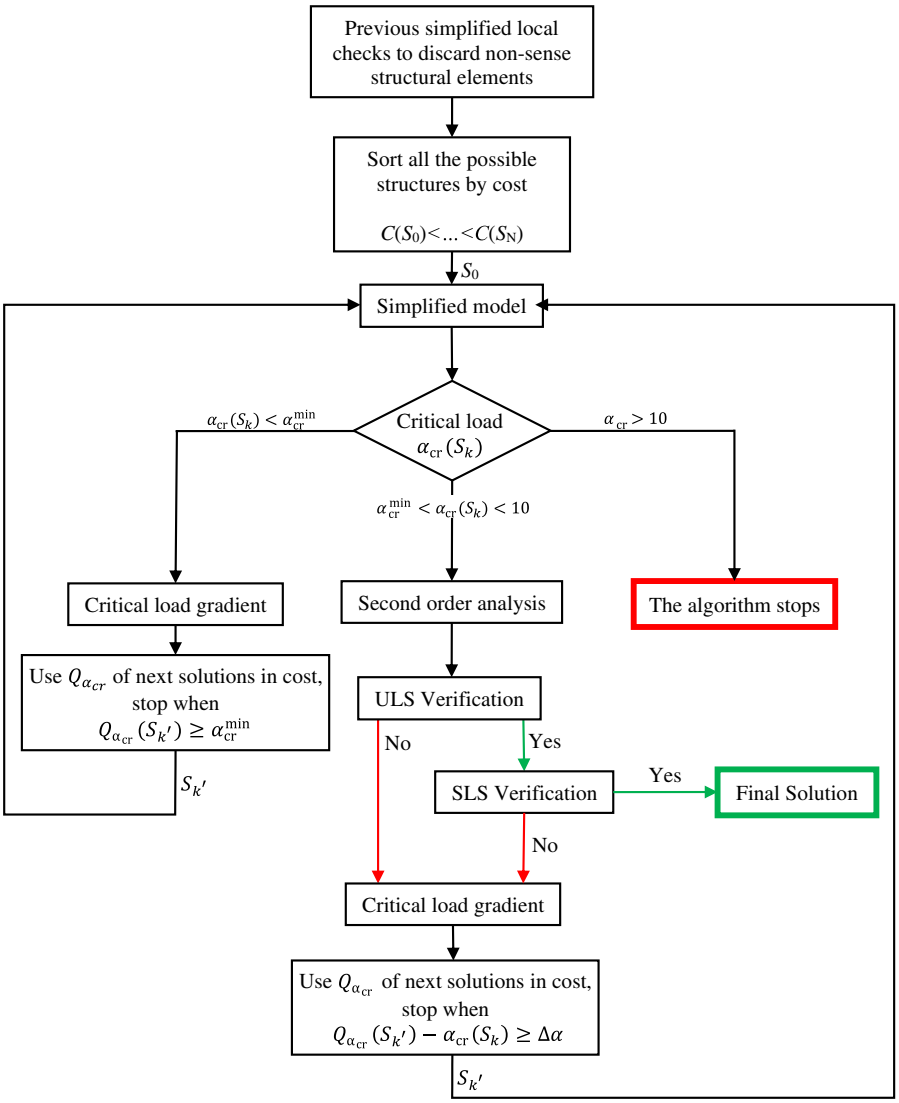

Fig. 3. Design algorithm flowchart.

J. Struct. Eng., 2020, 146(12): 04020276

solving the eigenvalue problem Eq. (3) of the single-column model. Then, depending on the value of the factor, a decision is made.

If the critical load factor is smaller than α_{cr}^{min}, no ULS or SLS analysis is performed. Instead, the linear critical load prediction Eq. (11) is used to find the cheapest solution S_k that fits the condition

$$Q_{\alpha_{cr}}(S_k) \geq \alpha_{cr}^{min} \tag{14}$$

Once a solution fulfilling Eq. (14) has been found, it is verified that the actual value of the critical load factor, determined from Eq. (3), is higher than α_{cr}^{min}. If it does not meet this condition, another solution $S_{k'}$ fitting Eq. (14) is checked. This time, the linear approximation departs from the structure $S_{k'}$. This process is repeated until finding the structure that fulfills $\alpha_{cr} \geq \alpha_{cr}^{min}$.

When in the structure S_k the critical load factor is greater than α_{cr}^{min} and smaller than 10, the corresponding second-order analysis Eq. (4) of the single-column model is solved. The resulting internal forces are used to perform the ULS and SLS checks. If S_k verifies the ultimate limit criteria, the algorithm stops. The best solution has been found. Conversely, if S_k fails, the next solution of the cost list, $S_{k'}$, the $Q_{\alpha_{cr}}(S_{k'})$ of which complies with Eq. (14) is studied, i.e., $S_{k'}$ goes through the whole verification loop from the beginning (Fig. 3).

To accelerate the process, the next solution $S_{k'}$ of the cost list is not actually analyzed; the idea is to choose a new solution for which a significant structural improvement is achieved. This new solution, $S_{k'}$, should comply $Q_{\alpha_{cr}}(S_{k'}) - \alpha_{cr}(S_k) \geq \Delta\alpha$; where $\Delta\alpha$ can be calibrated to ensure a significant improvement and a good prediction of $Q_{\alpha_{cr}}(S_{k'})$.

Finally, if $\alpha_{cr} > 10$, the global stability is not considered to play any relevant role, and, consequently, it does not make sense to carry out a design process based on the stability factor, as discussed previously. Thus, the algorithm stops.

In this process, often several structures that are evaluated have the same cost; the most stable structure is chosen.

Application Example

This section applies the design methodology to the rack structures in Figs. 4 and 5. These examples are carried out in two steps. First, the accuracy of the single-column model is assessed by comparing the results of a second-order analysis [according to Eq. (4)] with those produced by means of a full 2D beam finite-element model. Second, the proposed design procedure is applied and the resulting solutions are discussed.

In all the examples, the following profiles are considered: (1) uprights U_1–U_5, and (2) beams B_1–B_4. The properties of these profiles are given in Tables 2 and 3, respectively. These properties are similar to those of real profiles that can be found on the market. The cost (including manufacturing and erection) also is listed.

The stiffness of each upright-to-beam connection is given in Table 4. For simplification, only one upright base stiffness was considered, $K_f = 84$ kN · m/rad.

Example 1: Single-Column Model Verification

Linear buckling and second-order analyses were carried out on the structure of Example 1 by considering the cheapest configuration: U_1 for uprights, and B_1 for beams. All the beams were loaded with a gravity force of $Q = 14$ kN uniformly distributed along their length; no horizontal loading was considered other than that

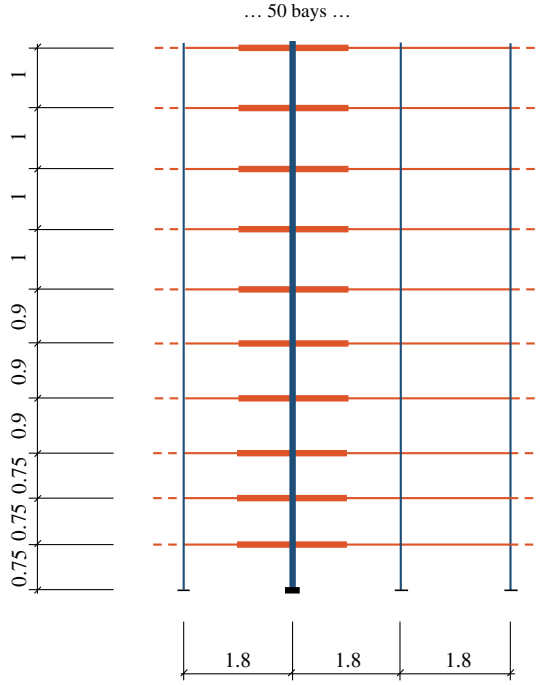

Fig. 4. Structure of Example 1.

corresponding to the sway imperfection. This load was calculated from (1) the out-of-plumb $\phi_{imp} = 0.002$ rad; and (2) the following looseness for each beam profile: for B_1, $\phi_{l1} = 0.001$ rad; for B_2, $\phi_{l2} = 0.00075$ rad; for B_3, $\phi_{l3} = 0.0006$ rad; and for B_4, $\phi_{l4} = 0.0006$ rad. Because only Upright U_1 was used in the example, only the looseness corresponding to the U_1–B_i connection was included herein. Both imperfections were combined according to EN 15512 (CEN 2009) to set the horizontal forces to be applied to the model.

The critical stability factors obtained in the analyses were $\alpha_{cr} = 1.230$ and $\alpha_{cr} = 1.235$ for the single-column and full 2D models, respectively; these values can be considered identical. The corresponding buckling modes also were very similar:

- Single-column model
  $\boldsymbol{\phi}_{cr}^{T} = \{0, 0.49, 1.11, 1.75, 2.46, 3.03, 3.42, 3.69, 3.85, 3.92, 3.97\}10^{-2}$ (Displacements)
  $\boldsymbol{\phi}_{cr}^{T} = -\{4.96, 7.28, 8.12, 7.94, 6.76, 4.97, 3.30, 1.93, 1.01, 0.51, 0.29\}10^{-6}$ (Rotations)
- Full 2D model
  $\boldsymbol{\phi}_{cr}^{T} = \{0, 0.49, 1.10, 1.74, 2.45, 3.01, 3.41, 3.69, 3.84, 3.92, 3.97\}10^{-2}$ (Displacements)
  $\boldsymbol{\phi}_{cr}^{T} = -\{4.89, 7.21, 8.07, 7.91, 6.77, 4.99, 3.34, 1.96, 1.04, 0.52, 0.30\}10^{-6}$ (Rotations)

The results of the second-order analysis of the single-column and the full models are compared in Tables 5–7 for an intermediate bay. Again, minor errors are observed concerning horizontal displacements, and beam and upright end moments. Slightly high differences occurred for some uprights with low bending moments, but they are not relevant from the design point of view.

If the number of bays decreases, the observed differences increase because the periodic nature of the structure is lost. However, the accuracy of results still can be considered reasonably good for predesign purposes for two reasons: (1) the safety of the final design is not compromised, because a further detailed verification is yet to be done, and (2) the most relevant elements for design purposes have the smallest differences in the comparison.

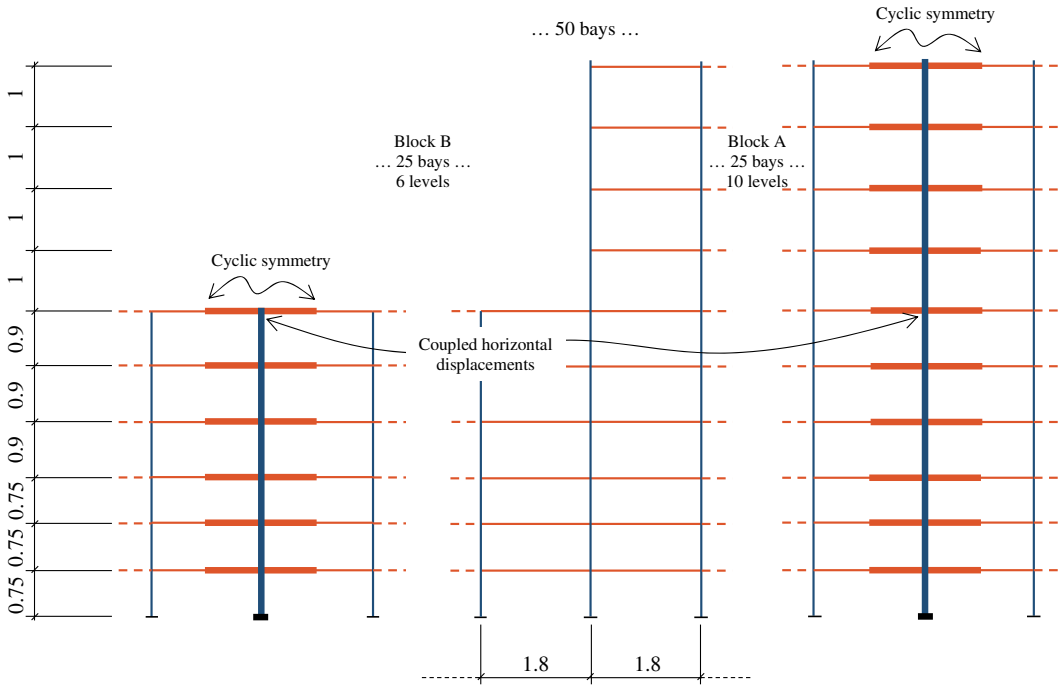

Fig. 5. Structure of Example 2.

Table 2. Beam properties

Beam	I_{eff} (mm^4)	W_{eff} (mm^3)	f_y (N/mm^2)	Cost (€/m)
B1	407,500	12,000	355	16.67
B2	600,000	15,000	355	26.33
B3	800,000	20,000	355	25.56
B4	100,000	25,000	355	28.88

Table 3. Upright properties

Upright	I_{eff} (mm^4)	W_{eff} (mm^3)	A_{eff} (mm^2)	f_y (N/mm^2)	Cost (€/m)
U1	400,000	10,000	360	355	55.87
U2	700,000	20,000	500	355	67.00
U3	1,200,000	30,000	560	355	80.45
U4	1,650,000	35,000	600	355	89.39
U5	1,750,000	40,000	720	355	111.73

Table 4. Beam-to-upright stiffness K_{u-b} (kN · m/rad)

	Beam			
Upright	B1	B2	B3	B4
U1	40	70	80	100
U2	60	80	90	120
U3	100	120	150	190
U4	150	160	175	220
U5	170	190	210	250

As expected, the accuracy of this model is higher for racks with many bays; fortunately, in such structures the provided savings are more important. For instance, Tables 8–10 (corresponding to a structure similar to that of Example 1, but with 15 bays) indicate that the relevant differences do not exceed 5%.

Table 5. Example 1: Regular example, displacements (%)

Level	Full model	Single column	Difference (%)
1	0.765	0.765	0.045
2	0.858	0.859	0.126
3	0.903	0.905	0.221
4	0.917	0.920	0.309
5	0.890	0.894	0.283
6	0.840	0.843	0.297
7	0.772	0.775	0.231
8	0.702	0.705	0.208
9	0.635	0.638	0.154
10	0.576	0.578	0.096

Example 1: Design Algorithm

The design algorithm was applied to Example 1 considering the following loading combinations:

- Ultimate limit state (ULS): $1.4(Q + Q_{\text{imp}})$; and
- Serviceability limit state (SLS): $(Q + Q_{\text{imp}})$.

The factor of 1.4 was set according to EN 15512 (CEN 2009). The initial solution (S_0) is the cheapest one, which was presented in the previous section. The chosen algorithm parameters were $\alpha_{\text{cr}}^{\text{min}} = 1.5$ and $\Delta\alpha = 0.0$ (Fig. 3). Noticeably, the chosen value of $\alpha_{\text{cr}}^{\text{min}}$ was rather low, and represented a potentially unstable situation; it did not fulfill some code design recommendations (CEN 2016a) for seismic situations. It was chosen because it is, to a certain extent, common in actual racks, and to analyze the performance of the proposed algorithm in such situations.

A valid solution was achieved after four iterations. Table 11 lists the resulting profiles and the cost of the structure. The same upright profile was used in all levels of the rack, as commonly occurs in practice. Consequently, Table 11 lists only one column for the upright solution. The results of the SLS and ULS verifications

Table 6. Example 1: Column moments (% of resistance moment)

	Node 1			Node 2		
Level	Full	Single column	Difference (%)	Full	Single column	Difference (%)
1	−18.22	−18.19	0.17	−2.51	−2.36	5.89
2	−14.12	−14.29	−1.19	−8.32	−8.29	0.34
3	−10.23	−10.34	−1.10	−10.47	−10.50	−0.25
4	−8.00	−8.08	−1.09	−12.97	−13.08	−0.84
5	−3.52	−3.51	0.11	−12.10	−12.20	−0.82
6	−0.99	−0.95	3.63	−9.61	−9.66	−0.57
7	−0.09	−0.08	12.92	−7.31	−7.34	−0.42
8	0.74	0.77	−3.73	−4.98	−4.99	−0.11
9	0.87	0.89	−1.96	−3.05	−3.05	−0.05
10	0.62	0.63	−2.36	−1.53	−1.51	1.30

Table 7. Example 1: Beam-end bending moments (% of resistance moment)

	Node 1			Node 2		
Level	Full	Single column	Difference (%)	Full	Single column	Difference (%)
1	17.66	17.68	0.09	−3.80	−3.80	0.03
2	18.47	18.50	0.19	−3.01	−2.98	1.14
3	18.44	18.48	0.24	−3.05	−3.00	1.64
4	17.61	17.65	0.25	−3.87	−3.83	1.13
5	16.19	16.22	0.16	−5.28	−5.26	0.49
6	14.79	14.80	0.07	−6.69	−6.68	0.19
7	13.48	13.48	0.01	−8.00	−8.00	0.02
8	12.45	12.45	−0.03	−9.03	−9.03	−0.05
9	11.75	11.75	−0.03	−9.72	−9.73	−0.13
10	11.39	11.37	−0.21	−10.12	−10.11	0.06

expressed in terms of utilization percentage are (maximum values within the structure):

- ULS: beams 98%; uprights 98%; joints 48%; and
- SLS: sway displacement 56%; beam deflection 64%.

The ULS verifications were carried out considering resistance values similar to real experimental values obtained from the tests in section "Pallet Rack Design."

The *SI* values of the different solution (S_i) were determined. Tables 12 and 13 list the *SI* values corresponding to the beam–upright joint stiffness and the beams, respectively. For the beams, higher values corresponded to the lower levels of the rack. This is consistent with the decisions of the design algorithm, which proposed upsizing those members on these levels showing the highest *SI* (Table 11). For the fourth iteration, this consistency did not occur. This was because, for solution S_4, the **H** term of the α approximation Eq. (11) is more relevant than the $\nabla\alpha$ term. The latter term is reflected directly in the SIs; conversely, the former is not. It is reasonable that such consistent results are obtained because (1) the solutions considered should have an increase in stability factor higher than the minimum $\Delta\alpha$, and consequently, solutions with low *SI* values are eliminated (in this example, however, $\Delta\alpha$ was equal to 0 and had no influence); and (2) when there is more than one solution with the same cost, the algorithm always selects the solution with the highest stability factor. For instance, in the second iteration (from S_2 to S_3) in Table 11, the cost of switching one B2 to B3 is the same for Levels 2 and 3, but, in the end, B3 is introduced in the third level because the resulting stability factor is higher than that of the other solution.

Table 8. Example 1 with 15 bays: Displacements (%)

Level	Full model	Single column	Difference (%)
1	0.770	0.765	0.454
2	0.808	0.859	4.148
3	0.853	0.905	4.414
4	0.870	0.920	4.382
5	0.847	0.894	3.915
6	0.801	0.843	3.356
7	0.739	0.775	2.706
8	0.673	0.705	2.138
9	0.610	0.638	1.686
10	0.554	0.578	1.328

This structure was designed following a conventional manufacturer's approach, and the resulting solution was compared with the one obtained with the methodology proposed herein. If the design process is not systematized and automated in some way, the option of changing the beam of only one level is not considered. This is because the amount of possible solutions is very high, and the selection process is very slow. For example, in this example, more than 5 million combinations are possible (of course, some of them do not make sense). Consequently, the same beam cross section was used in all levels.

When the conventional approach was applied to Example 1, the solutions first were sorted by cost. Afterward, as in the previous method, the initial solution was taken to be cheapest one, which did not satisfy the ULS and SLS design criteria. Then the next solution in terms of cost was studied: U_1 for the uprights, and B_2 for all beams. This solution was good, with $\alpha_{cr} = 1.83$ and the following utilization ratios:

- ULS: beams = 78%, uprights = 96%, and joints = 31%; and
- SLS: sway displacement = 45%, and beam deflection = 52%.

More-conservative values were obtained, but the final cost obviously was higher: €67,500. This structure was €8,400 more expensive per aisle, i.e., 14% more expensive (Table 11).

Table 9. Example 1 with 15 bays: Column moments (% of resistance moment)

	Node 1			Node 2		
Level	Full	Single column	Difference (%)	Full	Single column	Difference (%)
1	−18.22	−18.19	0.17	−2.51	−2.36	5.89
2	−14.12	−14.29	−1.19	−8.32	−8.29	0.34
3	−10.23	−10.34	−1.10	−10.47	−10.50	−0.25
4	−8.00	−8.08	−1.09	−12.97	−13.08	−0.84
5	−3.52	−3.51	0.11	−12.10	−12.20	−0.82
6	−0.99	−0.95	3.63	−9.61	−9.66	−0.57
7	−0.09	−0.08	12.92	−7.31	−7.34	−0.42
8	0.74	0.77	−3.73	−4.98	−4.99	−0.11
9	0.87	0.89	−1.96	−3.05	−3.05	−0.05
10	0.62	0.63	−2.36	−1.53	−1.51	1.30

Table 10. Example 1 with 15 bays: Beam-end bending moments (% of resistance moment)

	Node 1			Node 2		
Level	Full	Single column	Difference (%)	Full	Single column	Difference (%)
1	17.26	21.22	−2.46	−5.05	−4.56	9.60
2	18.08	22.21	−2.37	−4.09	−3.57	12.65
3	18.08	22.18	−2.25	−4.08	−3.60	11.88
4	17.33	21.18	−1.84	−4.97	−4.59	7.67
5	16.02	19.47	−1.26	−6.55	−6.31	3.68
6	14.69	17.76	−0.73	−8.15	−8.02	1.63
7	13.44	16.18	−0.33	−9.65	−9.60	0.53
8	12.44	14.94	−0.02	−10.85	−10.84	0.07
9	11.76	14.10	0.07	−11.65	−11.68	−0.24
10	11.41	13.64	0.32	−12.13	−12.13	−0.03

Table 11. Example 1: Evolution of design solution at iteration i of algorithm

				Beam at level										
S_i	Q_α	α_{cr}	Upright	1	2	3	4	5	6	7	8	9	10	Cost (€)
1	—	1.23	U1	B1	B1	B1	B1	B1	B1	B1	B1	B1	B1	55,500
2	1.50	1.49	U1	B1	B2	B2	B1	B1	B1	B1	B1	B1	B1	58,300
3	1.53	1.53	U1	B1	B2	B3	B1	B1	B1	B1	B1	B1	B1	58,700
4	1.56	1.57	U1	B1	B3	B3	B1	B1	B1	B1	B1	B1	B1	58,900
5	1.60	1.60	U1	B1	B4	B1	B2	B1	B1	B1	B1	B1	B1	59,100

Table 12. Example 1: Parameter sensitivity indicator for rotational spring stiffness, SI_r

	Level									
Iteration	1	2	3	4	5	6	7	8	9	10
1	19.76	24.55	23.49	17.05	9.19	4.06	1.38	0.38	0.10	0.03
2	19.42	14.98	14.85	20.59	15.95	9.00	3.66	1.14	0.31	0.10
3	17.25	12.00	12.45	21.22	18.65	11.39	4.90	1.57	0.43	0.15
4	20.45	14.67	13.24	19.87	16.38	9.62	4.02	1.27	0.35	0.12

Table 13. Example 1: Parameter sensitivity indicator for beam inertias, SI_m

	Level									
Iteration	1	2	3	4	5	6	7	8	9	10
1	19.76	24.55	23.49	17.05	9.19	4.06	1.38	0.38	0.10	0.03
2	17.29	18.84	18.67	18.33	14.20	8.02	3.26	1.01	0.27	0.09
3	19.19	19.45	12.90	18.64	15.37	9.03	3.78	1.20	0.33	0.11
4	17.09	12.34	12.80	21.03	18.47	11.28	4.85	1.56	0.43	0.15

Table 14. Example 1 ($\alpha_{cr}^{min} = 3$): Evolution of design solution at iteration i of algorithm

				Beam at level										
S_i	Q_α	α_{cr}	Upright	1	2	3	4	5	6	7	8	9	10	Cost (€)
1	—	1.23	U1	B1	B1	B1	B1	B1	B1	B1	B1	B1	B1	55,500
2	3.13	3.02	U2	B4	B4	B4	B4	B2	B2	B1	B1	B1	B1	71,200

As discussed previously, the value of $\alpha_{cr}^{min} = 1.5$ is rather low; therefore, this example also was worked using $\alpha_{cr}^{min} = 3$. The results are given in Table 14. Under this requirement, the algorithm reached a value of α_{cr} that was very close to the required value in only two steps, and that the upright and beams of the six lower levels were changed.

Example 2: Single-Column Model Verification

A second example show that the proposed single-column model and design algorithm can work properly when applied to rack structures with some kind of singularity in the down-aisle direction. The structure of Example 2 was the same as that of Example 1, except that the last four upper levels were removed from the first half of the rack (Fig. 5).

Table 15. Example 2: Displacements (%)

Block	Level	Full model	Single column	Difference (%)
A	1	0.63	0.64	1.57
	2	0.60	0.61	1.36
	3	0.57	0.58	1.15
	4	0.53	0.53	0.93
	5	0.48	0.49	0.75
	6	0.44	0.44	0.55
	7	0.40	0.40	0.44
	8	0.37	0.37	0.35
	9	0.34	0.34	0.28
	10	0.31	0.31	0.17
B	1	0.63	0.64	1.71
	2	0.60	0.61	1.41
	3	0.57	0.58	1.18
	4	0.53	0.53	0.97
	5	0.48	0.49	0.75
	6	0.44	0.44	0.65

The single-column model was applied to this structure, but in this example two columns were considered, one for each block of the rack (Fig. 5). The degrees of freedom and couplings of each column model were the same as those used in Example 1. However, additional couplings had to be added to link the two column models. The upright nodes at the same level of each model should have the same displacement (Fig. 5).

Linear buckling and second-order analyses were performed considering the same loading as in Example 1. The results of the analyses were compared with the results of a full 2D finite-element model. The critical stability factors obtained were $\alpha_{cr} = 1.384$ and $\alpha_{cr} = 1.377$ for the single-column model and full model, respectively. There was good agreement. The corresponding buckling modes also were similar

- Single-column model
  $\boldsymbol{\phi}_{cr}^{T} = \{0, 0.61, 1.17, 1.61, 2.00, 2.27, 2.43, 2.55, 2.62, 2.66, 2.68\}10^{-2}$ (Displacements)
  $\boldsymbol{\phi}_{cr}^{T} = -\{7.87, 7.53, 6.30, 4.90, 3.39, 2.16, 1.39, 0.85, 0.46, 0.23, 0.13\}10^{-6}$ (Rotations)
- Full model
  $\boldsymbol{\phi}_{cr}^{T} = \{0, 0.61, 1.16, 1.60, 1.99, 2.26, 2.43, 2.55, 2.62, 2.65, 2.67\}10^{-2}$ (Displacements)
  $\boldsymbol{\phi}_{cr}^{T} = -\{7.83, 7.50, 6.28, 4.90, 3.39, 2.17, 1.40, 0.86, 0.47, 0.24, 0.14\}10^{-6}$ (Rotations)

Tables 15–17 indicate reasonably good agreement with the results of the second-order analysis (large differences correspond to members with low bending moments).

A more sophisticated column model was tested in the study, which considered three columns: one column for the lower block, one column for the higher block, and one column for the transition from the lower to the higher blocks. The results obtained with this three-column model were somewhat worse than those of the two-column model. Therefore, the three-column model was discarded.

Table 16. Example 2: Column bending moments (% of resisting moment)

		Node 1			Node 2		
Block	Level	Full	Single column	Difference (%)	Full	Single column	Difference (%)
A	1	−6.73	−6.84	−1.63	−7.57	−7.77	−2.66
	2	−3.96	−3.91	1.22	−7.91	−8.12	−2.68
	3	−2.30	−2.21	4.01	−6.89	−7.06	−2.46
	4	−1.82	−1.71	6.32	−6.30	−6.41	−1.72
	5	−0.62	−0.57	9.02	−4.94	−5.17	−4.58
	6	−0.27	−0.06	77.56	−2.68	−2.58	3.55
	7	−1.59	−1.67	−4.91	−3.11	−3.18	−2.20
	8	−0.50	−0.43	14.67	−2.79	−2.79	−0.07
	9	0.17	0.17	−2.64	−1.96	−3.05	−2.57
	10	0.24	0.31	−26.75	−1.13	−1.51	2.96
B	1	−6.71	−6.82	−1.66	−7.47	−7.76	−3.75
	2	−4.04	−3.90	3.48	−8.01	−8.11	−1.24
	3	−2.22	−2.19	1.70	−6.97	−7.02	−0.72
	4	−1.74	−1.72	0.94	−6.36	−6.47	−1.71
	5	−0.57	−0.44	21.78	−4.94	−4.81	2.70
	6	−0.31	−0.43	−40.59	−3.90	−3.92	−0.53

Table 17. Example 2: Beam-end bending moments (% of resisting moment)

Block	Level	Node 1			Node 2		
		Full	Single column	Difference (%)	Full	Single column	Difference (%)
A	1	15.56	15.60	−0.22	5.90	5.88	0.20
	2	15.00	15.03	−0.20	6.46	6.45	0.06
	3	14.36	14.38	−0.12	7.09	7.10	−0.07
	4	13.61	13.63	−0.09	7.85	7.85	−0.05
	5	12.92	12.89	0.18	8.53	8.59	−0.67
	6	12.49	12.49	−0.07	8.87	8.98	−1.29
	7	12.24	12.23	0.05	9.21	9.25	−0.37
	8	11.84	11.82	0.19	9.64	9.66	−0.17
	9	11.45	11.44	0.07	10.02	10.04	−0.19
	10	11.23	11.20	0.27	10.29	10.28	0.09
B	1	15.54	15.60	−0.35	5.91	5.88	0.37
	2	15.00	15.03	−0.20	6.45	6.45	0.01
	3	14.37	14.38	−0.11	7.09	7.10	−0.09
	4	13.62	13.62	0.01	7.84	7.86	−0.25
	5	12.94	12.92	0.11	8.53	8.56	−0.24
	6	12.31	12.37	−0.54	9.13	9.11	0.31

Table 18. Example 2: Evolution of design solution of algorithm

			Block A										Block B							
			Beam at level										Beam at level							
S_i	Q_α	α_{cr}	Upright	1	2	3	4	5	6	7	8	9	10	Upright	1	2	3	4	5	6	Cost (€)
1	—	1.08	U1	B1	B1	B1	B1	B1	B1	B1	B1	B1	B1	U1	B1	B1	B1	B1	B1	B1	43,413
2	1.50	1.50	U1	B2	B1	B1	B1	B1	B1	B1	B1	B1	B1	U1	B2	B1	B1	B1	B1	B1	44,613
3	1.53	1.53	U1	B1	B1	B1	B1	B1	B1	B1	B1	B1	B1	U2	B1	B1	B1	B1	B1	B1	45,913
4	1.61	1.62	U1	B1	B1	B1	B1	B1	B1	B1	B1	B1	B1	U2	B2	B1	B1	B1	B1	B1	46,513

These results show that the proposed method can be applied to irregular structures provided that a sufficient number of columns are added to the single-column model, and appropriate boundary conditions are considered. Furthermore, simple nonuniform loading patterns, such as those required in EN 15512 (CEN 2009), also can be analyzed with this approach. However, if the structure or the load pattern are very irregular, the use of the single-column approach is not suitable because this single-column model would need a number of columns similar to that of the rack.

Example 2: Design Algorithm

Table 18 displays the results for Example 2. The final solution was:

1. In the first iteration (S_1–S_2), the stability increase was provided by upsizing the beams of the two first levels of the higher block (A).
2. In the second iteration (S_2–S_3), SI_m of the uprights of the lower (B) and higher (A) blocks was 49% and 51%, respectively. This means that, in terms of stability, it is slightly better to upsize the higher block uprights; however, that strategy is more expensive because the uprights are longer. Therefore, the lower block uprights were upsized instead.
3. In the third iteration (S_3–S_4), reinforcing the beams of the first level of Block B was more effective, because the stiffness of the U_2–B_i connections were higher than those of the U_1–B_i connections.

The utilization ratios of the resulting structure were:

- ULS: beams = 99%, uprights = 96%, and joints = 51%; and
- SLS: sway displacement = 88%, and beam deflection = 76%.

Conclusions

A simplified stability-based method for practical predesign of down-aisle unbraced selective racks was presented; only a single upright and its adjoining half beams were modeled, and were discretized with 2D bar elements. The proposed strategy is significantly faster than the conventional design approaches and yields less-expensive structures; in this sense, this paper shows that a design procedure based on improving the stability can lead to cost reduction.

The use of this method highlights the key role of beams in inexpensively improving the global stability (without upsizing all the beams), and can determine a final solution that might not be obvious.

Data Availability Statement

Some or all data, models, or code that support the findings of this study are available from the corresponding author upon reasonable request. Some or all data, models, or code generated or used during the study are proprietary or confidential in nature and may only be provided with restrictions.

Notation

The following symbols are used in this paper:

A = area;
C = condition (for SLS), cost;
E = demand (for ULS);
$\mathbf{F}$ = external force vector;

f = resistance (stress);
$\mathbf{H}$ = Hessian matrix;
H = coefficient of Hessian matrix;
I = moment of inertia;
$\mathbf{K}$ = stiffness matrix;
K = stiffness coefficient;
m = member;
N = axial force;
Q = variable (live) load, quadratic approximation;
R = resistance (for ULS);
S = design solution;
SIm = parameter sensitivity indicator for member;
SIr = parameter sensitivity indicator for rotational stiffness;
W = sectional modulus;
α = linear stability factor;
Δ = increment;
$\boldsymbol{\phi}$ = buckling mode, displacement vector;
ϕ = out-of-plumb angle, looseness angle; and
ψ = design parameter.

Subscripts and Superscripts

b = beam, buckling;
cr = critical;
d = design;
e = element;
eff = effective;
f = floor;
G = geometric;
i, k = numbers;
imp = imperfection;
j = joint, number;
l = looseness;
min = minimum;
n = number of elements;
r = rotational spring;
u = upright;
y = yielding; and
0 = initial.

References

AISI (American Iron and Steel Institute). 2016. *North American specification for the design of cold-formed steel structural members*. AISI S100-16. Washington, DC: AISI.

Bernuzzi, C., A. Gobetti, G. Gabbianelli, and A. Rosti. 2016. "Beam design for steel storage racks." *J. Const. Steel Res.* 116 (Jan): 156–172. https://doi.org/10.1016/j.jcsr.2015.09.007.

Bernuzzi, C., A. Gobetti, G. Gabbianelli, and M. Simoncelli. 2014. "Warping influence on the resistance of uprights in steel storage pallet racks." *J. Const. Steel Res.* 101 (Oct): 224–241. https://doi.org/10.1016/j.jcsr.2014.05.014.

Bernuzzi, C., A. Gobetti, G. Gabbianelli, and M. Simoncelli. 2015. "Simplified approaches to design medium-rise unbraced steel storage pallet racks. I: Elastic buckling analysis." *J. Struct. Eng.* 141 (11): 04015036. https://doi.org/10.1061/(ASCE)ST.1943-541X.0001271.

Bonada, J., M. Casafont, F. Roure, and M. M. Pastor. 2018. "Introduction of sectional constraints in a first-order GBT formulation for open-cross sections." In *Proc., 8th Int. Conf. on Thin-Walled Structures*. Lisboa, Portugal: Instituto Superior Técnico, Universidade de Lisboa.

Casafont, M., J. Bonada, M. M. Pastor, F. Roure, and A. Susin. 2017. "Linear buckling analysis of perforated cold-formed steel storage rack columns by means of the generalised beam theory." *Int. J. Struct. Stab. Dyn.* 18 (1): 1–32. https://doi.org/10.1142/S0219455418500049.

CEN (European Committee for Standardisation). 2002. *Basis of structural design*. EN 1990. Brussels, Belgium: CEN.

CEN (European Committee for Standardisation). 2004. *Design of steel structures. Part 1–5: Plated structural elements*. EN 1993-1-5. Brussels, Belgium: CEN.

CEN (European Committee for Standardisation). 2005. *Design of steel structures—Part 1-1: General rules and rules for buildings*. EN 1993-1-1. Brussels, Belgium: CEN.

CEN (European Committee for Standardisation). 2008. *Steel static storage systems—Adjustable pallet racking—Tolerances, deformations and clearances*. EN 15620. Brussels, Belgium: CEN.

CEN (European Committee for Standardisation). 2009. *Steel static storage system—Adjustable pallet racking systems—Principles for structural design*. EN 15512. Brussels, Belgium: CEN.

CEN (European Committee for Standardisation). 2016a. *Steel static storage systems—Adjustable pallet racking systems—Principles for seismic design*. EN 16681. Brussels, Belgium: CEN.

CEN (European Committee for Standardisation). 2016b. *Steel static storage systems—Adjustable pallet racking systems—Principles for structural design*. prEN 15512. Brussels, Belgium: CEN.

CEN (European Committee for Standardisation). 2019. *Design of steel structures—Part 1–3: General rules and rules—Supplementary rules for cold-formed members and sheeting (draft)*. EN 1993-1-3. Brussels, Belgium: CEN.

Cheng, B., and Z. Y. Wu. 2015. "Simplified method for calculating the lateral stiffness of drive-in storage racks." *Pract. Period. Struct. Des. Constr.* 21 (1): 04015008. https://doi.org/10.1061/(ASCE)SC.1943-5576.0000266.

Crosbie, M. W. J. 1998. "The design and analysis of static pallet racking systems." Master's thesis, Sheffield Hallam Univ.

Farkas, J., and K. Jarmai. 2013. *Optimum design of steel structures*. Berlin: Springer.

Godley, M. H. R. 2002. "The behaviour of drive-in storage structures." In *Proc., Int. Specialty Conf. on Cold-Formed Steel Structures*. Rolla, MO: Missouri Univ. of Science and Technology.

Hua, V., and K. Rasmussen. 2006. *The behaviour of drive-in racks under horizontal impact load*. Research Rep. No R871. Camperdown, NSW: School of Civil Engineering Sydney, Univ. of Sydney.

Liu, M. 2015. "Fast procedure for practical member sizing optimization of steel moment frames." *Pract. Period. Struct. Des. Constr.* 20 (4): 04014042. https://doi.org/10.1061/(ASCE)SC.1943-5576.0000240.

Manickarajah, D., M. Xie, and G. Steven. 2000. "Optimisation of columns and frames against buckling." *Comput. Struct.* 75 (1): 45–54. https://doi.org/10.1016/S0045-7949(99)00082-6.

Mueller, M., M. Liu, and S. Burns. 2002. "Fully stressed design of frame structures and multiple load paths." *J. Struct. Eng.* 128 (6): 806–814. https://doi.org/10.1061/(ASCE)0733-9445(2002)128:6(806).

Nocedal, J., and S. J. Wright. 2006. *Numerical optimization*. 2nd ed. New York: Springer.

Perelmuter, A., and V. Slivker. 2001. "The problem of interpretations of the stability analysis results." In *Proc., European Conf. on Computational Mechanics*. Cracow, Poland: Dept. of Technical Sciences of the Polish Academy of Sciences Polish Association for Computational Mechanics Cracow Univ. of Technology.

Sena, F., and K. Rasmussen. 2016. "Finite element (FE) modelling of storage rack frames." *J. Const. Steel Res.* 126 (Nov): 1–14. https://doi.org/10.1016/j.jcsr.2016.06.015.

Szalai, J. 2010. "Use of eigenvalue analysis for different levels of stability design." In *Proc., SDSS'Rio 2010 Stability and Ductility of Steel Structures*. Rio de Janeiro, Brazil: Coppe/Federal Univ. of Rio De Janeiro.

Tilburgs, K. 2013. "Those peculiar structures in cold-formed steel: 'Racking & shelving'." *Steel Const. Des. Res.* 6 (2): 95–106. https://doi.org/10.1002/stco.201310016.

Trouncer, A., and K. Rasmussen. 2016. "Ultra-light gauge steel storage rack frames. Part 2—Analysis and design considerations of second order effects." *J. Const. Steel Res.* 124 (Sep): 37–46. https://doi.org/10.1016/j.jcsr.2016.05.015.